Optical Engineering 44(5), 051102 (May 2005)

Picosecond high-repetition-rate pulsed laser ablation of dielectrics: the effect of energy accumulation between pulses

Barry Luther-Davies
Andrei V. Rode
Nathan R. Madsen
Eugene G. Gamaly
ARC Centre for Ultra-high Bandwidth Devices for Optical Systems
Australian National University
Research School of Physical Science and Engineering
Laser Physics Centre
Canberra, ACT 0200, Australia
E-mail: bld111@rsphysse.anu.edu.au

Abstract. We report experiments on the ablation of arsenic trisulphide and silicon using high-repetition-rate (megahertz) trains of picosecond pulses. In the case of arsenic trisulphide, the average single pulse fluence at ablation threshold is found to be >100 times lower when pulses are delivered as a 76-MHz train compared with the case of a solitary pulse. For silicon, however, the threshold for a 4.1-MHz train equals the value for a solitary pulse. A model of irradiation by high-repetition-rate pulse trains demonstrates that for arsenic trisulphide energy accumulates in the target surface from several hundred successive pulses, lowering the ablation threshold and causing a change from the laser-solid to laser-plasma mode as the surface temperature increases. © *2005 Society of Photo-Optical Instrumentation Engineers.* [DOI: 10.1117/1.1905363]

Subject terms: pulsed laser ablation; laser-induced damage; laser applications.

Paper 040547 received Aug. 12, 2004; revised manuscript received Oct. 25, 2004; accepted Nov. 18, 2004; published online May 25, 2005.

1 Introduction

Pulsed laser deposition (PLD), when applied in its conventional form using low-repetition-rate lasers emitting nanosecond-range pulses,[1] generally leads to poor-quality films contaminated by particles. As a result, the method is not normally useful when films of the highest optical quality are required such as for the fabrication of optical waveguides. It has been shown that particle contamination can, however, be a direct consequence of the use of the conventional pulse parameters[2] that lead to a large volume of material being evaporated by each pulse. The plume so-produced expands as a supersaturated vapor and, therefore, condenses during the early stage of the expansion, resulting in the formation of droplets from the vapor phase. These are then deposited onto the substrate.

A solution to droplet formation has been found with better insight into the physics of the laser ablation process. It has been shown that droplets can be eliminated by changing the mode of operation of the laser.[2,3] Similar average laser powers are employed, but the energy is delivered in shorter pulses (10 to 100 ps rather than ≈10 ns), containing around six orders of magnitude lower energy (microjoules rather than joules) but at much higher repetition rates (≈10 MHz rather than ≈10 Hz). We call this mode of operation ultrafast pulsed laser deposition (UFPLD). Each single short low-energy high-intensity pulse evaporates relatively few ($\sim 10^{11}$ to 10^{12}) atoms per pulse,[2,3] thereby inhibiting the condensation of droplets during the fast nonequilibrium expansion. To compensate for the reduced ablated mass per pulse, high pulse repetition rates are used to achieve a high average deposition rate. The high repetition rate maintains the average atomic flow in a plume at a high level of 10^{19} to 10^{20} atoms/s.

0091-3286/2005/$22.00 © 2005 SPIE

The ultrafast laser ablation method has already been applied to produce atomically smooth, diamond-like carbon films[2,3] with total elimination of macroscopic particles from the film surface. Recently, As_2S_3 chalcogenide optical films[4] were produced with similar surface quality and high homogeneity. A simple method to produce a flat ''top-hat'' intensity distribution over the focal spot has been proposed and implemented for the deposition of high surface quality silicon films using femtosecond pulses from a Ti:sapphire laser.[5] However, many parameters must be controlled that affect the quality of the films produced by UFPLD, including the laser intensity distribution on the target surface, the scanning speed of the laser focal spot over the target, the repetition rate of the laser, the energy level of the prepulse and postpulse, the pressure of any reactive gas in the experimental chamber, and the physical properties of the target material. Hence, a thorough understanding is needed of the interaction mode and the effect of various parameters on the creation of the laser-ablated plume. Many experimental and theoretical studies of the ablation rate of solids with ultrashort pulses indicate the presence of two different ablation regimes, depending on the pulse duration,[6–14] with the transition between these regimes occurring for pulses in the tens of picoseconds range. Thus, the laser-target interaction physics for pulse durations between a few hundred femtoseconds and a few tens of picoseconds is such that in both cases, nonequilibrium processes must be taken into account. It is the purpose of this paper to elucidate the interaction physics in conditions near the ablation threshold when high-repetition-rate trains of picosecond pulses are used such that many successive pulses hit the same spot on the target surface.

For most of our experimental work on UFPLD we used ≈10- to 100-ps-duration pulses as opposed to femtosecond pulses for a number of practical reasons. Our major goal has been to develop UFPLD for depositing optical wave-

guide quality glass films rapidly over very large areas (>0.5 m^2). This inevitably requires high average power lasers and systems based on neodymium-doped crystals offer the best average power scalability. This situation has changed very recently following the development of thin-disk, ≈a hundred femtosecond, mode-locked Yb lasers producing >60 W of average power.[15] Neodymium lasers can be efficiently converted to higher (or lower) frequencies using second-order nonlinear optical processes. Thus, neodymium-based systems offer the advantages of high average power, power scalability, short pulses, near diffraction-limited beam quality, and frequency agility.

We recently reported a new ablation laser based on a master oscillator power amplifier system using the combination of a variable repetition rate Nd:YVO_4 oscillator producing about 3 W of average power and a Fraunhofer Innoslab Nd:YVO_4 power amplifier, which boosts the average output at 1064 nm into the 40- to 50-W range.[16] This system delivers 13-ps pulses at repetition rates as high as 28 and as low as 1.5 MHz in a near-diffraction-limited beam ($M_x^2<1.2; M_y^2<1.4$). Additionally we used a commercial Coherent Antares mode-locked Nd:YAG laser producing around 20 W at 1064 nm in ≈60-ps pulses at a 76-MHz repetition rate in our experiments. For both lasers, external frequency doubling using noncritically phase matched LBO crystals generated between 6 and 40 W quasi-cw power at 532 nm.

In this paper, we primarily describe the interaction physics for the case of arsenic trisulphide chalcogenide glass, but also include for comparison some results for silicon. For these materials, the cooling time of the laser-irradiated surface can be relatively long (up to several tens of microseconds) and comparable with the time between successive pulses. Hence, irradiation with a high-repetition-rate pulse train can result in different interaction physics compared with the case of metals where the cooling time is[17] <100 ps. As a result, it is possible that the energy from several pulses accumulates in the focal spot, raising the surface temperature in a stepwise fashion. This is certainly the case for chalcogenide glass, where we observe that when pulses are delivered as a high-repetition-rate pulse train, ablation occurs at single pulse fluences orders of magnitude below the threshold expected for a solitary pulse.

We develop a model that considers that coupling between the successive pulses gradually increases the surface temperature and eventually transforms the laser-matter interaction into a regime where much stronger laser-target coupling occurs. Therefore, the first m pulses that hit the same spot on the target (from the total number of N pulses/spot) do not lead to ablation but heat the surface progressively until a threshold condition is reached. The remaining $N-m$ pulses then produce ablation since the conditions at the surface exceed this threshold. This situation applies in particular to ultrafast ablation of chalcogenide glasses. The case of silicon is more complex because its physical properties change drastically with temperature and hence the laser-heated surface can behave very differently from that predicted by the properties at room temperature. As a result, accumulation in silicon is a small effect and we observe that the threshold for ablation by a high-repetition-rate pulse train is close to the reported single pulse value.

The analysis presented in this paper is aimed specifically at the case of nonmetals—metals themselves behave qualitatively differently and are dealt with elsewhere.[17] Nonmetals have two important properties. First, at low intensity, their absorption is moderate and hence the absorbed energy is distributed over a relatively thick layer of material. This requires some clarification since to achieve ablation at all, the material must strongly absorb the incident light and, therefore, the laser wavelength is generally chosen to be below the band edge of the material. In nonmetals, values of complex dielectric constant at wavelengths close to, but below, the band edge generally correspond to absorption lengths of a few micrometers. These are relatively large compared with the case for metals where absorption occurs in a skin layer only 30 to 40 nm thick. Second, these materials have poor thermal conductivity, again in comparison with metals. As a result, the time gap between the pulses from a laser producing a megahertz pulse train can be too short for complete cooling of the irradiated spot between successive pulses (as shown later, the cooling time for As_2S_3 chalcogenide glass ≈35 μs). Since the speed at which the beam can be scanned over the surface using mechanical scanners is limited, this means many hundreds or even thousands of pulses will hit the same spot on the target. Thus, the laser irradiates a spot already heated by the previous pulses and the surface temperature gradually rises in a stepwise fashion until it reaches a value sufficient for thermal evaporation.

However, this is not the end of the story because once thermal evaporation begins, it becomes possible for the laser-target coupling to change markedly. After the onset of thermal evaporation, the temperature continues to grow near the target surface as does the vapor density in front of that surface. At a sufficiently high temperature, the vapor becomes partially ionized, and this leads to a change in the laser-matter interaction mode from absorption in a layer whose thickness is determined by the dielectric properties of the solid, to stronger and more localized absorption on a plasma density gradient. The absorption length in the plasma is comparable with the skin depth in a metal, and the local temperature at the critical surface thus increases abruptly. This makes it possible to reach the threshold for nonthermal ablation, which is the normal process that occurs when single picosecond or subpicosecond pulses are used to ablate solids.[6–14] Therefore, ablation can occur due to both nonequilibrium processes during the pulse and thermal evaporation after the pulse. Thus, when using high-repetition-rate pulse trains, the temperature at the sample surface is determined not only by the single pulse parameters but also by the time the beam ''dwells'' at a single point. This can result in complex changes in the nature of the laser-target interaction.

Such accumulation effects using high-repetition-rate lasers have already been noticed during ablation of carbon by a 76-MHz-repetition-rate laser.[2] The effects of high-repetition-rate ablation, including cumulative heating, have been observed in ablation and deposition of chalcogenide glasses.[4] Cumulative heating in the bulk of transparent glass has also been reported.[18]

In this paper, we mainly focus on the ablation of As_2S_3 chalcogenide glass using a 76-MHz Antares laser although some results on the ablation of silicon targets using a 4.1-

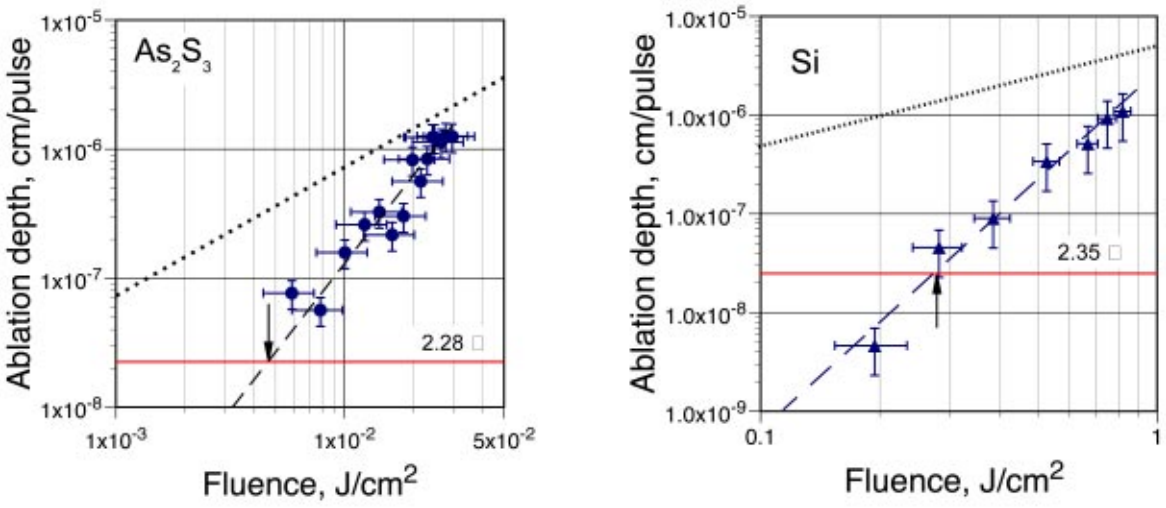

Fig. 1 (a) Ablation depth for As_2S_3 measured as a function of fluence. The horizontal line represents the thickness of a monolayer of As_2S_3 in angstroms; the dotted line represents the maximum ablation depth from energy conservation conditions assuming 100% absorption; the threshold as defined in the text is shown by the arrow. (b) Equivalent data for Si.

MHz pulse train from the high-power mode-locked Nd:YVO_4 laser are also included. We analyze the experiments using a model that examines the conditions and consequences of energy accumulation and compare its predictions with the experimental data. We conclude that accumulation dominates the interaction between the 76-MHz pulse train and the As_2S_3, while for silicon, the rapid change in material properties with temperature results in the interaction mode remaining in the single-pulse regime.

2 Experimental Results

We summarize here the results of experiments on ablation of chalcogenide glass (As_2S_3) and single-crystal silicon performed using megahertz-repetition-rate lasers. The first experiments involved ablation of As_2S_3 chalcogenide glass in vacuum using the 76-MHz-repetition-rate coherent Antares laser. The maximum pulse energy used in these experiments was 70 nJ and could be varied by changing the pump power of the laser. The output beam was frequency doubled using a noncritically phase matched lithium triborate crystal and focused onto the samples using a 300-mm-focal-length lens. The focal spot was measured by reimaging it onto a CCD camera using a microscope objective and had a beam diameter (FWHM) of 15 μm. The area of the focal spot was thus fixed at $s_{\mathrm{foc}}=1.8\times10^{-6}\,\mathrm{cm}^2$ and the beam was scanned over a line ≈6 mm long on the target surface at 555 Hz using an oscillating mirror. The average ablation depth per pulse [Fig. 1(a)] was determined from measurements of the volume of the crater formed in the target using a profilometer divided by the total number of pulses that hit the target (7.6×10^5). The error bars indicate the variance in values obtained for multiple measurements in the same conditions and estimates of the accuracy to which the absolute fluence was determined from the experimental measurements.

Since the focal spot diameter (≈15 μm) was much larger than optical absorption depth, which at 532 nm is ≈few 10^{-4} cm for As_2S_3 ablation can be considered to be a 1-D process. The fluence at the ablation threshold can be determined by extrapolating the ablation depth dependence to the zero depth, such as it was used in a number of reports.[3,19,20] However, it appears that the threshold obtained in this manner may depend strongly on the extrapolation procedure since the fluence dependence is not a simple linear function. Moreover, there is no physically reasonable scenario describing a process that results in the random removal of only a few of the surface atoms that must then occur as the zero ablation depth is approached. Therefore, it seems justifiable to define the ablation threshold as the average pulse fluence required to remove a single atomic surface layer. The horizontal line in Fig. 1 represents the approximate thickness of a single atomic layer for As_2S_3 of 2.28 Å. As is apparent from Fig. 1(a) the threshold for removing a single atomic layer is extremely low ≈5 mJ/cm^2 and this is well below the predicted single pulse ablation threshold for As_2S_3 (see later). The ablated volume per pulse also approaches the maximum value predicted from energy conservation [Sec. 2.2—dotted line in Fig. 1(a)] at fluences of only ≈20 mJ/cm^2. We therefore conclude that in As_2S_3, the accumulation of energy between pulses within the pulse train must have a major effect.

The second experiments involved ablation of silicon using a 4.1-MHz-repetition-rate pulse train. The single crystal Si samples were exposed[16,21] in vacuum to 25 to 28 W of average power from the mode-locked frequency-doubled Nd:YVO_4 laser at 532 nm with the energy per pulse on the target surface $E_p=6.5\,\mu$J, the pulse duration $t_p=13$ ps, and the repetition rate 4.1 MHz. In this case, the energy per pulse and pulse duration were fixed, while the focal area was varied by moving the target surface relative the focus of the $f=300$ mm lens in the range from $S_{f,\mathrm{min}}=5\times10^{-6}\,\mathrm{cm}^2$ ($d_f=25\,\mu$m FWHM) to $S_{f,\mathrm{max}}=1.2\times10^{-4}\,\mathrm{cm}^2$ ($d_f=124\,\mu$m). This corresponds to fluences from 1.3 to 5.4×10^{-2} J/cm^2 and intensities from 1.0×10^{11} to 4.2×10^9 W/cm^2.

The laser beam was again scanned over a region approximately 17×13 mm. The amount of material ablated during a 60-s exposure was measured by weighing the sample with an accuracy $\pm 10^{-4}$ g before and after the ablation. The ablated mass per single pulse m_{av} was determined by averaging the mass difference over the 2.46×10^8 pulses.

The data for these experiments are shown in Fig. 1(b). The focal spot diameter was again much larger than optical absorption depth, which at 532 nm is $\approx 2\times 10^{-4}$ cm for crystalline silicon and ≈100 nm for amorphous silicon[22] and, hence, ablation can be considered to be a 1-D process. The horizontal line in Fig. 1(b) represents the thickness of a single atomic layer for Si of 2.35 Å. As is evident the ablation threshold is close to 0.3 J/cm^2, which is consistent with values of the ablation threshold using short pulses reported previously.[23] This suggests that the experiments in silicon appear to be little affected by the use of the high-repetition-rate pulse train and ablation occurs at close to conditions for a solitary pulse.

2.1 *Scanning Conditions: Dwell Time and Number of Pulses per Focal Spot*

Many laser pulses arrive at the same spot on the target surface because the scanning speed is too low to physically separate the beam from successive pulses when the repetition rate is in the 1- to 100-MHz range. Since the scanners employed produced sinusoidal patterns, one can easily estimate the maximum $t_{\max}$ and minimum $t_{\min}$ time that the laser beam ''dwells'' over a focal spot of a diameter d_f for a given scanning frequency ω_s, repetition rate R_{rep}, and a scanning area of a size a.

The laser beam spends maximum time near the beam turning points because the scanning velocity passes through zero while changing direction and because the beam crosses the same spot twice. For 1-D scanning the maximum dwell time is expressed as follows ($\omega_s t_{\max} \ll 1$):

$$t_{\max} = \frac{4}{\omega_s}\left(\frac{d_f}{a}\right)^{1/2}. \tag{1}$$

Similarly, the minimum dwell time near the center of the line is

$$t_{\min} = \frac{2 d_f}{a\,\omega_s}. \tag{2}$$

In the ablation experiments of As_2S_3 using the 76-MHz-repetition-rate laser ($d_f = 15\ \mu$m; $a \sim 6$ mm; $\omega_s \sim 3487$ rad/s) the number of pulses per spot lay in the range ≈342 to 4400. Similarly for the silicon ablation using the 2-D scanning ($\omega_s \sim 371$ to 383 rad/s, $a \sim 15$ mm, $d_f = 25$ to 124 μm, $R_{\mathrm{rep}} = 4.1$ MHz) the number of laser pulses per spot varied from ≈36 in the middle at the maximum fluence to $\approx 3.95\times 10^3$ at the turning points for the lowest fluence. Therefore ablation by high-megahertz-repetition-rate lasers using ~100-Hz scanners, numerous pulses interact with the same spot, which can make the interaction regime drastically different from the single-pulse case.

2.2 *Ablated Mass and Depth*

The ablated mass per pulse m_{av} was determined by dividing the total mass lost by the total number of pulses that hit the target. The ablation depth per pulse was then calculated using:

$$l_{\mathrm{abl}} = \frac{m_{\mathrm{av}}}{S_f \rho}, \tag{3}$$

where ρ is the target mass density, and S_f is the focal spot area.

Note that energy conservation defines an upper limit to the mass that can be ablated (or equivalently the maximum depth ablated) to create a fully atomized plume by a single pulse with an energy E_p (fluence F_p) as follows:

$$l_{\mathrm{abl}}^{\max} = \frac{F_p M_a}{\epsilon_b \rho}, \tag{4}$$

$$m_{\mathrm{abl}}^{\max} = \frac{E_p M_a}{\epsilon_b}, \tag{5}$$

where M_a is the atomic mass, and ϵ_b is the binding energy. Equations (4) and (5) assume total absorption, i.e., $A = 1$. The values are plotted in Figs. 1(a) and 1(b) and are significantly higher than the experimental data. This indicates that the measured data are physically reasonable, and that the difference can be explained by incomplete absorption by the target ($A < 1$); energy lost to bulk heating or in the kinetic energy of the expanding plume.

3 Discussion and Analysis

The laser energy is primarily absorbed by electrons, which then transfer their energy to the lattice (phonons). The electron-phonon energy exchange rate can be estimated[24] as follows: $v_{e-\mathrm{ph}} \approx (J_i/\hbar)(m_e/M)$. Here J_i is the ionization potential. One can see that for silicon ($J_i = 8.15$ eV and $M = 28.086$ au) this time is ≈4 ps. A similar estimate gives the electron-lattice equilibration time for chalcogenide glass between 1.2 and 3.7 ps (sulphur: $J_i = 10.36$ eV and $M = 32$ au; arsenic: $J_i = 9.81$ eV and $M = 74.92$ au). Thus, equilibration of the electron and lattice temperatures occurs before the end of the pulse for durations in the range 10 to 60 ps, as used in our experiments. Hence, the single temperature approximation is a valid description of heating and ablation and is used in further analysis. Before proceeding, we note also that it is well established that laser ablation can proceed via two mechanisms: nonthermal ablation occurs if the lattice temperature exceeds that corresponding to the binding energy of the material; while if the lattice temperature is below the binding energy, then equilibrium evaporation can take place. Hence, the temperature in the absorbing layer is a crucial parameter defining the nature of the laser-material interaction.

3.1 *Temperature in the Absorbing Layer*

Let us estimate the temperature induced by a single pulse in the absorbing layer. The maximum temperature induced by a single laser pulse can be estimated assuming that the losses due to material expansion and heat conduction are

Table 1 Optical properties of silicon and chalcogenide glasses at $\lambda=532$ nm ($\omega=3.54\times10^{15}\,s^{-1}$).

	Crystalline Si	Amorphous Si	As_2S_3
n	4.15	4.43	2.6
κ	0.044	0.876	0.04
l_{abs} (cm)	1.924×10^{-4}	9.66×10^{-6}	2×10^{-4}
A	0.626	0.586	0.8
D (cm^2/s)	0.907	0.907	1.15×10^{-3}
Binding energy (eV)	4.118		~2.2

negligible. In fact, as demonstrated later, the heat penetration depth $l_{th}=(Dt_p)^{1/2}$ (D is heat diffusion coefficient and t_p is the pulse duration) during the pulse for chalcogenide glass is insignificant compared with the absorption length and small even in the most unfavorable estimates for silicon. Thus, the maximum temperature in the absorbing layer can be estimated as follows[14]:

$$T_m=\frac{2AF_p}{C_L l_{abs} n_a}, \tag{6}$$

where C_L, n_a, and A are, respectively, the lattice specific heat, the atomic density, and the absorption coefficient; $l_{abs}=(c/\omega\kappa)$ is the absorption length (ω is the laser light frequency, κ is the imaginary part of the refractive index, and c is the speed of light in vacuum); and $F_{t=tp}=F_p$ is the total fluence of the laser pulse of duration t_p.

In experiments using the Antares laser to ablate As_2S_3, a single pulse [532 nm, $A=0.8$, $l_{abs}=2.1\times10^{-4}$ cm, $n_a=0.39\times10^{23}\,cm^{-3}$, and $C_L=3.73\times10^{-23}$ J/K (Ref. 25)] results in a temperature increase per pulse only $\Delta T=26$ K at 5×10^{-3} J/cm^2, while the average ablation depth of $\sim10^{-6}$ cm/pulse was derived from the experiments! Such a small temperature rise is too small to cause any changes in the optical properties of As_2S_3 and completely rules out any role for thermal evaporation for a single pulse at the threshold fluence. Hence the use of the 76-MHz pulse train must result in a dramatic increase in the ablation rate relative to the single-pulse case, indicating a strong role for accumulation effects.

The situation with silicon is more complex because its dielectric and thermal properties are strong functions of temperature. For example, at room temperature the parameters for single crystal silicon[22] correspond to $l_{abs}=1.92\times10^{-4}$ cm and $A=0.63$ at 532 nm. At the threshold fluence of $F_p=0.3$ J/cm^2, this gives a surface temperature of 1190 K, which is below the melting temperature ($T_m=1883$ K). Thus, at first sight ablation by a single pulse of crystalline silicon should not occur and certainly nonthermal ablation would not be expected.

In the experiments, however, the laser beam was scanned continuously over the surface and hence the irradiated surface is modified (amorphized) by many successive pulses and is likely to change from its initial crystalline state. Amorphous silicon possesses optical properties closer to those of metals,[22] and it has lower thermal diffusivity of 0.13 cm^2/s than crystalline silicon (see Table 1). If we therefore use the optical parameters of amorphous silicon, we find that a single pulse of 532-nm laser light at 0.3 J/cm^2 heats amorphous silicon ($l_{abs}=97$ nm; $A=0.58$) to the temperature of 2.2×10^4 K (1.89 eV), which is well in excess of boiling temperature ($T_{boil}=2628$ K) and therefore is sufficient for thermal evaporation but still less than the binding energy. Note that in the preceding estimates, we took into account only the lattice heat capacity considering that all newly transferred into the conduction band electrons are degenerate.

To further complicate the situation, the optical and thermal properties of crystal silicon are strongly temperature dependent. For example, by 1200 K, κ has[26] increased to $\kappa\approx0.37$,[29] corresponding to a change in absorption length l_{abs} from $\approx10^{-4}$ cm to $\approx2\times10^{-5}$ cm—closer to the value for amorphous silicon. Furthermore, at the melting temperature it was reported that Si has already transformed into a metallic state characterized by four conducting electrons,[27] in which case, $\kappa\approx5.3$, $l_{abs}\approx16$ nm, $A\approx0.3$, and the temperature rises to $\approx10^5$ K (8.6 eV), which is greater than the binding energy. Hence, it is difficult to assign constants for the optical parameters of an irradiated silicon surface. As a result, although the very first pulse at the threshold energy of 0.3 J/cm^2 may only just reach the melting temperature of crystalline silicon, the energy delivered to the surface is sufficient to transform it from a crystalline to an amorphous state. The following pulse is then able to drive the system to much higher temperatures and in fact reach the nonthermal ablation threshold where $T\geqslant\epsilon_b$. As a result, it becomes unlikely that it would be necessary to invoke any accumulation effects to explain the measured threshold.

3.2 *Single-Pulse Ablation Threshold*

The nonequilibrium ablation threshold is defined as follows[14]:

$$F_{abl}^{n\text{-}eq}=\frac{C_L n_a \epsilon_b l_{abs}}{2A}, \tag{7}$$

which corresponds to the condition that the average energy of the atoms equals the binding energy. We assume that the heat capacity near the nonequilibrium ablation threshold (temperature~binding energy) has attained a value close to that of an ideal gas $C_L=1.5k_B$. The nonequilibrium ablation threshold at 532 nm for amorphous silicon is then 0.4 J/cm^2, which is very close to the observed value considering the uncertainty associated with the complex behavior of silicon at the elevated temperature already noted. On the other hand, the nonequilibrium ablation threshold for chalcogenide glass ($A=0.8$, $l_{abs}=2.1\times10^{-4}$ cm, $C_L=1.5k_B$, $\epsilon_b=2.2$ eV, and $n_a=0.39\times10^{23}\,cm^{-3}$) equals 2.7 J/cm^2—orders of magnitude higher than the observed multipulse threshold of 5 mJ/cm^2. Thus, the ablation of chalcogenide glass can proceed only by thermal evaporation.

The thermal evaporation rate is expressed as follows[28]:

$$(nv)_{therm}\approx n_0\left(\frac{2T}{M}\right)^{1/2}\exp\left(-\frac{\epsilon_b}{T}\right). \tag{8}$$

The threshold for thermal ablation using our definition can be defined using Eq. (8) by setting the total number of atoms removed from the material equal to that in a monoatomic surface layer:

$$\int_0^{t_{\rm th}} (nv)_{\rm therm}\,{\rm d}t \approx n_0\, d_a\,. \tag{9}$$

This definition now can be applied to the ablation during the pulse and after the end of the pulse. One can also use Eq. (9) in the case of multiple-pulse action if the time dependence of the temperature is known.

3.3 *Temperature Accumulation During Multiple-Pulse Irradiation*

The primary mechanism that leads to coupling between successive pulses in dielectrics, such as chalcogenide glasses, is due to a steady increase in the temperature with an increasing number of pulses. Cooling between the pulses is small if the heat conduction is sufficiently slow. The growth in temperature can be estimated as follows. Let us assume that the temperature drops after the end of the first pulse due to 1-D linear heat conduction (because $l_{\rm th} \ll l_{\rm abs} \ll d_f$). Hence,

$$T = T_1 \left(\frac{t_{\rm th}}{t_{\rm th} + R_{\rm rep}^{-1}} \right)^{1/2} \equiv \alpha T_1\,. \tag{10}$$

The characteristic cooling time $t_{\rm th}$ of the absorbing layer with thickness $l_{\rm abs}$ is $t_{\rm th} = l_{\rm abs}^2/D$. Here D is thermal diffusivity in square centimeters per second. The time gap between the successive pulses is $(R_{\rm rep})^{-1}$. One can see that the condition $\alpha \leqslant 1$ always holds. The temperature rise after the N'th pulse hitting the same spot then can be written in the form

$$T_N = T_1(1 + \alpha + \alpha^3 + \cdots + \alpha^N) = T_1 \frac{1-\alpha^N}{1-\alpha}. \tag{11}$$

Let's consider the example of As_2S_3, where heat conduction is slow and the absorption depth moderate. The relevant parameters are $D = 1.15 \times 10^{-3}\,{\rm cm}^2/{\rm s}$, $l_{\rm abs} = 2 \times 10^{-4}\,{\rm cm}$, and $t_{\rm th} = 3.48 \times 10^{-5}\,{\rm s}$. Thus, the cooling time is very much larger than the interpulse spacing, and in these conditions, the temperature in the absorbing layer grows as $T_N \sim N \times T_1$ until the thermal ablation threshold is reached.

3.4 *Thermal Ablation Threshold for Multiple Pulses*

The ablation threshold can be calculated if the dependence of the temperature on time is known. In conditions when accumulation is strong, the temperature grows in a stepwise manner, being practically constant between the pulses. The temperature in the absorbing layer after the N'th pulse is then expressed as $T_N = 293\,{\rm K} + N\Delta T_1$. The total thermal ablation depth to the end of N'th pulse can be presented as a sum of contributions from all previous pulses as follows:

$$l_{\rm thermal} = \frac{1}{n_0} \int_0^{t_{\rm th}} (nv)_{\rm therm}\,{\rm d}t = \sum_{m=1}^{N} \left(\frac{2T_m}{M} \right)^{1/2} \exp\left(-\frac{\epsilon_b}{T_m} \right) R_{\rm rep}^{-1}. \tag{12}$$

It is convenient to introduce a relative temperature $\theta_N = T_N/T_1$ and present Eq. (12) in the form

$$l_{\rm thermal} = v_1 R_{\rm rep}^{-1} \sum_{m=1}^{N} \theta_m^{1/2} \exp\left(-\frac{\epsilon_b}{T_1 \theta_m} \right) \approx v_1 R_{\rm rep}^{-1} \int_1^{\theta_N} \theta^{1/2} \exp\left(-\frac{\epsilon_b}{T_1 \theta} \right) {\rm d}\theta. \tag{13}$$

The threshold is reached after N pulses when the sum of the ablation depths for all pulses up to the N'th equals the thickness of the monoatomic layer $l_{\rm thermal} \approx d_a$. Numerical solution of Eq. (13) produces $\theta_N = T_N/T_1 \sim 7.2$ for ablation of chalcogenide glass by the 76-MHz Antares laser ($\epsilon_b/T_1 = 80$, $R_{\rm rep} = 76\,{\rm MHz}$, $T_1 = 26\,{\rm K} + 293\,{\rm K} = 0.0275\,{\rm eV}$, $d_a \sim 2.5 \times 10^{-8}\,{\rm cm}$, $v_1 \sim 10^5\,{\rm cm/s}$). Thus, the ablation threshold can be reached due to temperature accumulation from $N_{\rm thr} = (T_{N_{\rm thr}}/T_1)(293\,{\rm K}/\Delta T_1 + 1) - (293\,{\rm K}/\Delta T_1) \sim 77$ pulses. This is far fewer than the average number of pulses hitting a single spot in most regions of the target determined in Sec. 2.1. Hence, we can conclude that accumulation of the energy in the focal spot from irradiation by a large number of pulses can explain the ablation threshold observed in the experiments and that material removal commences as thermal evaporation at a temperature well below the binding energy.

3.5 *Change in the Interaction Regime*

In the experiments using the 76-MHz laser we concluded from the preceding reasoning that after several tens of pulses, the temperature at the ablation surface increases to about 0.2 eV, which is sufficient for thermal evaporation and indicates why the ablation threshold occurs at the extraordinarily low single-pulse value of 5 mJ/cm^2.

Generally in the experiments, many more pulses hit the same spot of the target (as many as 10^4) than required, simply to reach the threshold for thermal evaporation. Furthermore, the fluence used in the experiments was generally several times (two to four) the threshold value. This has two consequences. First, the temperature will continue to rise beyond the ''threshold'' temperature of 0.2 eV as more pulses hit the target until an equilibrium is established where the losses associated with plume expansion and thermal conduction balance the energy inflow from the laser. Since thermal conduction remains insignificant until more than 3000 pulses have arrived at the same spot on the target, the surface temperature can rise well above the minimum value and can approach ≈ 1 eV. Second, the rate of rise of the surface temperature will be two to four times faster than that corresponding to irradiation at the threshold fluence, meaning that even for the smallest dwell time (≈ 180 pulses), the surface temperature can rise well above the minimum value for thermal evaporation.

As the temperature approaches 1 eV, the characteristics of the laser-surface interaction can change markedly. At such a temperature, which is about one tenth of the ionization potential for arsenic and sulphur, ionization becomes significant (~10%) and both the solid surface and the vapor plume in front of the target converts into plasma.[29] Thus, the incident laser light will be absorbed on the plasma density gradient rather than at the solid interface. Let us estimate the conditions for the efficient absorption in plasma. We approximate the electron density gradient in plasma near the solid-plume interface by a linear profile, $n_e = n_c(x/L)$ with characteristic space scale L (n_c is the critical density for the incident laser radiation). The absorption in plasma will be significant when $[Lv_{ei}(n_c)]/3c > 1$ (Ref. 30). Here $v_{ei}(n_c)$ is the characteristic electron-ion collision rate taken at the critical density, and c is speed of light in vacuum. One can see that to have significant absorption in plasma in the conditions of the experiments, the plasma at a density equal to the critical density must be only about 0.1 μm thick [$v_{ei}(n_c) \sim 8\times10^{15}\,\mathrm{s}^{-1}; n_c \sim 4\times10^{21}\,\mathrm{cm}^{-3}$]. Even after one pulse, the vapor density at a distance of 0.1 μm from the surface would be larger than the critical density, assuming adiabatic expansion occurs after the end of the pulse. Therefore, we can expect that the vapor very near the target surface will be ionized and of sufficient density for the laser-matter interaction to change to the laser-plasma mode.

When this change occurs, the absorption is localized at the plasma critical density surface and this significantly increases the temperature in the absorbing region. The temperature can be estimated assuming that whole absorption occurs at the critical density:

$$M_a n_c v^3 \approx AI, \quad v = \left(\frac{2T}{M_a}\right)^{1/2}. \tag{14}$$

Then the temperature reads

$$T_e \approx \frac{M_a}{2}\left(\frac{I_{\mathrm{abs}}}{M_a n_c}\right)^{2/3}. \tag{15}$$

Thus, during ablation of As_2S_3 glass ($M_{av}=49$) by the Antares laser at $I=2.65\times10^8\,\mathrm{W/cm^2}$ ($\approx 16\,\mathrm{mJ/cm^2}$) using $A=0.8$, a single pulse interacting in the laser-plasma mode increases the temperature at the critical surface by 2.8 eV, which is slightly larger than the binding energy. As a result, ablation can then proceed by the nonequilibrium mechanism with a maximum ablation depth per pulse $l_{\mathrm{abl}}^{\max} = (F_p M_a/\epsilon_b \rho)$, which is close to the values observed in the experiments. This more efficient mode of ablation continues until the beam moves to the next point on the target surface and may be the dominant mechanism since up to several thousand pulses hit the same spot.

4 Conclusions

The presented experimental results and analysis demonstrate that evaporation of chalcogenide glass using high-repetition-rate 76-MHz lasers occurs even when the energy in each pulse is several orders of magnitude below that required for nonthermal ablation. This is due to the fact that the glass has very low thermal diffusivity ($\sim 2\times10^{-3}\,\mathrm{cm^2/s}$), which means that the energy from as many as 3000 pulses can accumulate in the surface before cooling due to thermal conduction becomes significant. In fact, when megahertz-repetition-rate lasers are used for ablation and when the focused beam is scanned over the target using mechanical mirror scanners, up to several thousand pulses hit the same spot on the target surface. The accumulation of energy from consecutive pulses results in the laser material interaction proceeding in several stages.

First, the temperature rises in a stepwise fashion due to accumulation of energy from successive pulses. Eventually, the surface temperature reaches the value where thermal evaporation becomes significant. At a fluence of only 5 $\mathrm{mJ/cm^2}$ at 532 nm, 77 pulses are required to reach this threshold, which occurs when the surface temperature reaches 0.2 eV for As_2S_3 glass. This is many fewer pulses than even the smallest number (340) that hit the same spot on the target in our experiments. Even once thermal evaporation has started, the surface temperature continues to rise until the energy in-flow is balanced by energy losses due to heat conduction and plume expansion. At $\approx$1 eV, the surface and vapor temperatures are sufficient to convert to the plume into the plasma state. Thus, the laser-material interaction changes to the laser-plasma mode, with absorption localized in a region $\approx$100 nm thick near the critical density surface. This localization increases the rise in temperature caused by a single pulse to $\approx$2.8 eV, which is close to the binding energy of the atoms at the surface. This change to the laser-plasma interaction mode results in efficient material removal by nonthermal ablation during the pulse, which adds to the material removed by thermal evaporation after the pulse. This scenario appears to describe the experiments on the ablation of chalcogenide glass using the 76-MHz laser.

In the case of silicon, the behavior is different and there is little evidence that accumulation plays any role because the measured multipulse ablation threshold using a 4.1-MHz pulse train is very close to the single-pulse values reported by other workers. The dependence of the dielectric constants of silicon on temperature leads to conversion of the solid silicon surface to a solid density plasma during a single pulse, and this results in energy being confined within a thin skin layer at the surface. The behavior then mirrors that of metals where nonthermal ablation dominates and the surface cools rapidly between pulses, eliminating the possibility of energy accumulation even at high repetition rates.

Thus, we conclude that accumulation of energy from many pulses in a high-repetition-rate pulse train can lead to strong ablation of materials with poor thermal conductivity at pulse energies well below the threshold for a solitary pulse. This behavior must be taken into account when evaporating materials such as chalcogenide glasses since it leads to conditions in the plume that differ markedly from those achieved using single pulses. It is important to understand the processes when depositing high-quality films of dielectrics using UFPLD.

Acknowledgments

The support of the Australian Research Council through its Centre of Excellence and Federation Fellowship programs is gratefully acknowledged.

References

1. D. B. Chrisey and G. K. Hubler, Eds., *Pulsed Laser Deposition of Thin Films*, Wiley, New York (1994); J. C. Miller and R. F. Haglund, Jr., Eds., *Laser Ablation and Desorption*, Academic Press, San Diego, CA (1998).
2. E. G. Gamaly, A. V. Rode, and B. Luther-Davies, *J. Appl. Phys.* **85**, 4121–4213 (1999); A. V. Rode, B. Luther-Davies, and E. G. Gamaly, *J. Appl. Phys.* **85**, 4222–4230 (1999).
3. M. D. Perry, B. C. Stuart, P. S. Banks, M. D. Feit, V. Yanovsky, and A. M. Rubenchik, *J. Appl. Phys.* **85**, 6803–6810 (1999).
4. A. V. Rode, A. Zakery, M. Samoc, E. G. Gamaly, and B. Luther-Davies, *Appl. Surf. Sci.* **197–198**, 481–485 (2002).
5. E. G. Gamaly, A. V. Rode, O. Uteza, B. Luther-Davies, T. Bauer, F. Korte, and B. Chikov, *J. Appl. Phys.* **95**, 2250 (2004).
6. P. B. Corkum, F. Brunel, N. K. Sherman, and T. Srinivasan-Rao, *Phys. Rev. Lett.* **61**, 2886–2889 (1988).
7. B. C. Stuart, M. D. Feit, S. Herman, A. M. Rubenchik, B. W. Shore, and M. D. Perry, *J. Opt. Soc. Am. B* **13**, 459–468 (1996).
8. S. Nolte, C. Momma, H. Jacobs, A. Tünnermann, B. N. Chichkov, B. Wellegehausen, and H. Welling, *J. Opt. Soc. Am. B* **14**, 2716–2722 (1997).
9. D. Du, X. Liu, G. Korn, J. Squier, and G. Mourou, *Appl. Phys. Lett.* **64**, 3071–3073 (1994).
10. B. C. Stuart, M. D. Feit, A. M. Rubenchik, B. W. Shore, and M. D. Perry, *Phys. Rev. Lett.* **74**, 2248–2251 (1995).
11. M. Malvezzi, N. Bloembergen, and C. Y. Huang, *Phys. Rev. Lett.* **57**, 146–149 (1986).
12. B. Luther-Davies, E. G. Gamaly, Y. Wang, A. V. Rode, and V. T. Tikhonchuk, *Sov. J. Quantum Electron.* **22**, 289–325 (1992).
13. K. Eidmann, J. Meyer-ter-Vehn, T. Schlegel, and S. Huller, *Phys. Rev. E* **62**, 1202–1214 (2000).
14. E. G. Gamaly, A. V. Rode, B. Luther-Davies, and V. T. Tikhonchuk, *Phys. Plasmas* **9**, 949 (2002).
15. E. Innerhofer, T. Sudmeyer, F. Brunner, R. Haring, A. Aschwanden, R. Paschotta, C. Honninger, M. Kumkar, and U. Keller, *Opt. Lett.* **28**, 367 (2003).
16. B. Luther-Davies, V. Z. Kolev, M. J. Lederer, N. R. Madsen, J. Giesekus, K.-M. Du, and M. Duering, *Appl. Phys. A: Mater. Sci. Process.* **79**, 1051 (2004).
17. E. G. Gamaly, A. V. Rode, N. R. Madsen, B. Luther-Davies, V. Z. Kolev, and M. Duering, *Phys. Rev. B* (to be published).
18. C. B. Schaffer, J. F. Garcia, and E. Mazur, *Appl. Phys. A: Mater. Sci. Process.* **76**, 351 (2003).
19. B. C. Stuart, M. D. Feit, S. Herman, A. M. Rubenchik, B. W. Shore, and M. D. Perry, *J. Opt. Soc. Am. B* **13**, 459–468 (1996).
20. S. Nolte, C. Momma, H. Jacobs, A. Tünnermann, B. N. Chichkov, B. Wellegehausen, and H. Welling, *J. Opt. Soc. Am. B* **14**, 2716–2722 (1997).
21. V. Z. Kolev, M. J. Lederer, B. Luther-Davies, and A. V. Rode, *Opt. Lett.* **28**, 1275 (2003).
22. E. D. Palik, Ed., *Handbook of Optical Constants of Solids*, Academic Press, New York (1985).
23. P. P. Pronko, P. A. VanRompay, C. Horvath, F. Loesel, T. Juhasz, X. Liu, and G. Mourou, *Phys. Rev. B* **58**, 2387 (1998); J. Bonse, S. Baudach, J. Krüger, W. Kautek, and M. Lenzner, *Appl. Phys. A: Mater. Sci. Process.* **74**, 19 (2002).
24. Y. A. Il'insky and L. V. Keldysh, *Electromagnetic Response of Material Media*, Plenum Press, New York (1994).
25. M. A. Popescu, *Non-Crystalline Chalcogenides*, Kluwer, Academic Publishers (2000).
26. J. Sìk, J. Hora, and J. Humlicek, *J. Appl. Phys.* **84**, 6291 (1998).
27. P. M. Fauchet and K. D. Li, *J. Non-Cryst. Solids* **97–98**, 1267–1270 (1987).
28. L. D. Landau and E. M. Lifshitz, *Statistical Physics*, Pergamon Press, Oxford (1980).
29. Y. B. Zel'dovich and Y. P. Raizer, *Physics of Shock Waves and High-Temperature Hydrodynamic Phenomena*, Dover, New York (2002).
30. W. L. Kruer, *The Physics of Laser Plasma Interaction*, Addison Wesley, New York (1987).

Barry Luther-Davies heads the Laser Physics Center at the Australian National University. His interests include laser-matter interaction physics, nonlinear optical materials and phenomena, photonics and ultrafast lasers, and he has published around 250 papers in these fields. He received his BSc degree in electronics in 1970 and his PhD degree in nonlinear optics in 1974, both from the University of Southampton, United Kingdom. He is currently a federation fellow funded by the Australian Research Council at the Australian National University in Canberra.

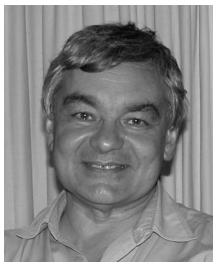

Andrei V. Rode graduated from the Moscow State University in 1975 and received his PhD degree from the Lebedev Institute of Physics of the Russian Academy of Sciences in 1986. In 1989 he joined the Laser Physics Center at the Australian National University, where he is now a senior fellow. His research interests are in short-pulse laser-matter interaction, laser ablation, laser-induced phase transitions, laser-produced nanoclusters and their properties, and laser deposition of nonlinear optical films.

Nathan R. Madsen is a PhD student working on ultra-fast-pulsed laser ablation of various materials, for example, chalcogenide glasses, metals, and carbon. His PhD project involves the controlled creation of carbon nanofoam involving the use of *in situ* plume diagnostics combined with postdeposition characterization. Photograph not available.

Eugene G. Gamaly graduated from the Moscow State University in 1958 with an MS degree in theoretical physics, received his PhD degree in 1970 from Federal Nuclear Center, Russia, and became a professor of physics with P.N. Lebedev Physical Institute of Russian Academy of Sciences, Moscow, in 1980. He worked within the research team of Prof. N. G. Basov, Nobel Prize winner, during the period 1973 to 1992 and was involved in pioneering research on laser-induced fusion and on the basics of laser-matter interactions. His recent research includes laser-induced phase transitions, ablation and deposition of thin films, and formation of nanostructures and their properties. He has published more than 300 papers in refereed journals, books, and book chapters.